ECMWF RE-ANALYSIS

ERA-40 Project Report Series

5. Analyses and forecasts of stratospheric winter polar vortex break-up: September 2002 in the Southern Hemisphere and related events from ECMWF operations and ERA-40

Adrian Simmons, Mariano Hortal, Graeme Kelly,
Anthony McNally, Agathe Untch and Sakari Uppala

European Centre for Medium-Range Weather Forecasts
Europäisches Zentrum für mittelfristige Wettervorhersage
Centre européen pour les prévisions météorologiques à moyen terme

For additional copies contact:

The Library
ECMWF
Shinfield Park
Reading, Berks RG2 9AX

library@ecmwf.int

Series: ERA40 Project Report Series

A full list of ECMWF Publications can be found on our web site under: http://www.ecmwf.int/publications/

ERA-40 project report series no.5

Analyses and forecasts of stratospheric winter polar vortex break-up: September 2002 in the southern hemisphere and related events from ECMWF operations and ERA-40

Adrian Simmons, Mariano Hortal, Graeme Kelly, Anthony McNally, Agathe Untch and Sakari Uppala

Research Department

March 2003

ABSTRACT

Break-up of the polar stratospheric vortex in the northern hemisphere is an event that is known to be predictable for up to a week or so ahead. This is illustrated using ERA-40 reanalysis data for the sudden warmings of January 1958 and February 1979, and operational ECMWF data for February 2003. It is then shown that a similar level of skill was achieved in operational forecasts for the split of the southern stratospheric vortex in late September 2002. The highly unusual flow conditions nevertheless exposed a computational instability of the forecast model. Analyses and forecasts from reruns using improved versions of the forecasting system are presented. Isentropic maps of potential vorticity and specific humidity provide striking pictures of the advective processes at work. Forecasts as well as analyses are shown to be in good agreement with radiosonde measurements of the temperature changes associated with vortex movement, distortion and break-up during August and September. Forecasts from 17 September onwards capture the remarkable temperature rise of about 60^{o}C recorded at 20hPa by the Halley radiosonde station as the vortex split. Objective forecast verification and data-denial experiments are used to characterize the performance of the observing and data-assimilation systems and to infer overall forecast, analysis and observation accuracy. The observations and analyses from 1957 onwards in the ERA-40 archive confirm the extreme nature of the 2002 event. Secondary vortex development by barotropic instability is also discussed.

1 Introduction

Towards the end of September 2002, the cold polar vortex in the southern hemisphere stratosphere elongated and split in a manner similar to that seen every few years in the northern hemisphere stratosphere, but never before observed in the southern hemisphere. Despite its rarity, the event was predicted accurately up to about a week in advance by the operational ECMWF forecasting system. Although the forecasts were successful, the unusual flow conditions exposed a weakness in the numerical stability of the forecast model. Improved results, in terms both of reduced noise and of slightly increased forecast accuracy, have been obtained in reruns of the data assimilation and forecasts which span August, September and part of October. The resulting high-resolution reanalyses provide a resource for future studies of the exceptional Antarctic stratospheric winter of 2002. The impact of different components of the observing system on analysis and forecast accuracy has been studied in further runs of the forecasting system for this period.

In this report we illustrate and discuss the performance of the ECMWF forecasting system for this event, and use the analyses and observations from the ERA-40 reanalysis project to help to put the event in context. A summary of the versions of the forecasting system used operationally and for ERA-40 is given in the next section. Section 3 provides an introductory discussion of forecasting-system performance in cases of similar vortex break-up and sudden warming in the northern hemisphere. Section 4 presents operational analyses and forecasts of the September 2002 event in the southern hemisphere. Computational stability is discussed in Section 5 and reruns of the data assimilation and forecasts in Section 6. One of the reruns is examined in further detail in Section 7 in terms of the accuracy of the analyses and forecasts, and the impact of the satellite and radiosonde components of the observing system. Section 8 reports on a search through the ERA-40 archives to check for any indications of similar behaviour in earlier years. Secondary vortex development by barotropic instability is discussed in Section 9 and concluding remarks are made in section 10.

2 The ECMWF forecasting system

The operational ECMWF medium-range forecasting system is based on a global atmospheric model with comprehensive parametrizations of physical processes, tightly coupled with an ocean-wave model. In its highest-resolution application the atmospheric model is run with a spherical-harmonic horizontal representation that since November 2000 has been truncated triangularly at wavenumber 511. The corresponding computational grid has an almost uniform spacing of just under 40km. Variables are represented at 60 levels in the vertical, ranging from a height of 10m above the surface to a pressure of 0.1hPa (a height of about 65km). Vertical resolution is approximately uniform in height with a spacing of about

1.5km in the middle stratosphere between 70hPa and 3hPa. This model is used for data assimilation and to produce deterministic high-resolution forecasts to ten days ahead. Ensembles of perturbed lower-resolution medium-range forecasts are also run operationally to provide probabilistic predictions, using T255 spectral resolution and a 40-level vertical resolution extending only to 10hPa. The (unperturbed) control forecasts of 10hPa height for the austral stratosphere in September 2002 from this ensemble system, although reasonably skilful, were generally not as accurate as the 60-level operational forecasts. All operational forecasts presented here are from the higher-resolution version of the model.

An incremental four-dimensional variational data assimilation (4D-Var) is used to produce initial conditions for the medium-range forecasts. Corrections to 12-hour high-resolution background forecasts for 00 and 12UTC (analysis increments) are derived using a T159-resolution version of the model to optimize the fits of forecasts to *in-situ* and remotely-sensed observations taken in the time windows 15-03UTC and 03-15UTC. Of the types of data used, temperature and wind measurements from radiosondes and radiances from the satellite-borne AMSU-A microwave sounding instruments have the most direct influence on the middle stratospheric analysis, with the radiance data predominant in the extratropical southern hemisphere, as will be seen later. Radiance data are assimilated directly; changes to the background model fields are sought that minimize the mis-match between simulated model-based radiances and measured values.

Results will be presented from two versions of the operational forecasting system. The first, referred to as cycle 25r1, is that operational in September 2002. The second, cycle 25r4, superseded cycle 25r1 for operational use in January 2003. The change included improvements to the physical parametrizations of the model, improvements to the formulation of the 4D-Var analysis, and the assimilation of several new types of satellite data. During September 2002, AMSU-A data from instruments on two satellites (NOAA-15 and NOAA-16) were assimilated operationally, while data from the newly-launched NOAA-17 satellite were under assessment. NOAA-17 data have been used in operations in addition to data from NOAA-15 and NOAA-16 since late October 2002. They have been used also in two of the reruns for August and September 2002 discussed in this report.

In the ERA-40 project, observations made in the period from August 1957 to June 2002 have been reanalysed using a six-hourly three-dimensional variational version (3D-Var) of the ECMWF data-assimilation system. The assimilating model used a coarser T159 spectral truncation, but the full operational 60-level vertical resolution. The data assimilation was based on an earlier cycle (23r4) of the forecasting system operational in the second half of 2001, modified to include a few newer features subsequently used operationally in cycles 25r1 and 25r4. Ten-day forecasts have been produced from each of the 00UTC and 12UTC ERA-40 analyses for selected years, employing the model version used for the ERA-40 data assimilation.

A substantial documentation of the operational and ERA-40 data-assimilation systems, including extensive references, may be viewed on the ECMWF website (http://www.ecmwf.int). Reference will be made below to specific papers of particular relevance to the present study.

3 Analyses and forecasts of northern hemispheric vortex break-up

Fifty years prior to the remarkable September 2002 event in the southern hemisphere, Scherhag(1952) reported an equally remarkable and never-before observed warming of more than 40^{o}C over two days measured at heights above 30km by radiosondes launched from Berlin late in February that year. Originally dubbed “The Berlin Phenomenon”, it subsequently became clear that such “sudden warmings” are by no means rare in the northern hemisphere winter stratosphere, and can be associated with substantial changes in

the large-scale circulation pattern. On occasions these changes comprise simply distortion, growth or decay, or a spatial shift of the principal features of the wintertime stratospheric circulation, namely the cold polar vortex and the Aleutian anticyclone. Once every few years, however, the vortex elongates and splits substantially or completely into two, often accompanied by development of a second anticyclone.

Three examples of such vortex break-up are presented here. These cases have not been specially chosen because they exhibit an unusually high level of forecast skill. Rather, two are well-known cases from the past that can now be reexamined using the ERA-40 analyses and forecasts, and the third is simply the latest occurrence, in February 2003, as captured by the operational ECMWF forecasting system. In each case 10hPa height analyses are presented for a date on which the vortex was split and for five and nine days earlier, together with forecasts of the vortex split made five, seven and nine days ahead. The nine-day range is the farthest ahead at which some indication of splitting, albeit weak, is seen in all three cases.

The first example from ERA-40, shown in Fig. 1, is from January 1958. Scherhag(1960) referred to this case as a recurrence of the Berlin Phenomenon after the passing of six years. The 10hPa analysis of geopotential height for 20 January shows a substantial cyclonic vortex centred well off the pole between northern Norway and Greenland, accompanied by a quite strong Aleutian anticyclone. Four days later, the planetary-wave pattern has rotated eastward, the vortex has assumed a more elongated and bowed shape and high pressure has built over southern and eastern Europe. By 29 January, the vortex has split completely into two separate vortices, one centred over Canada and one over Russia. Anticyclones are located over the Bering Strait and southwest of Ireland. The evolution depicted in these 10hPa ERA-40 analyses matches well that seen in 25hPa analyses reported at the time by Teweles and Finger(1958) and by Scherhag(1960).

The five-day forecast for 29 January is clearly successful in capturing the vortex split, the principal error being a slight eastward shift of the overall pattern, a shift evident also in the seven- and nine-day forecasts for this date. Apart from the shift, each of these forecasts represents quite well the twin anticyclones and main cyclonic centre over Russia. The treatment of the weaker vortex over Canada is, however, increasingly poor with increasing forecast range. Nevertheless, all forecasts out to day six show complete splitting of the vortex, in the sense that no closed contour line encompasses both low centres in height maps such as those shown. The radiosonde measurements (which include soundings from fixed ocean weather ships) and conventional surface observations from 1958 evidently permit remarkably good forecasts of this major stratospheric warming, when processed by a skilful modern data-assimilation system.

The second example from ERA-40, presented in Fig. 2, is the event that occurred in February 1979. Although there are differences in the size and orientation of the polar vortex as analysed for 12 and 16 February 1979 compared with 20 and 24 January 1958, the subsequent vortex break-up results in a pattern on 21 February 1979 that is similar to that of 29 January 1958. The situation on 21 February can be seen to be forecast accurately at five-day range, but there is a quite rapid decline in skill beyond six days ahead.

This 1979 event has been much studied (see Jung *et al.* (2001), and references therein). ECMWF first produced analyses for the period as part of its contribution to the First GARP[1] Global Experiment (FGGE). Forecasts run from the FGGE analyses by Bengtsson *et al.*(1982) and Simmons and Strüfing(1983) provided highly accurate depictions not only of the February vortex split but also of the major circulation changes that occurred in preceding weeks. This was the first time such forecast skill had been demonstrated for

1. Global Atmospheric Research Programme

stratospheric warming events, although some degree of success had been reported some years earlier in pioneering experiments by Miyakoda *et al.* (1970) for the case of March 1965.

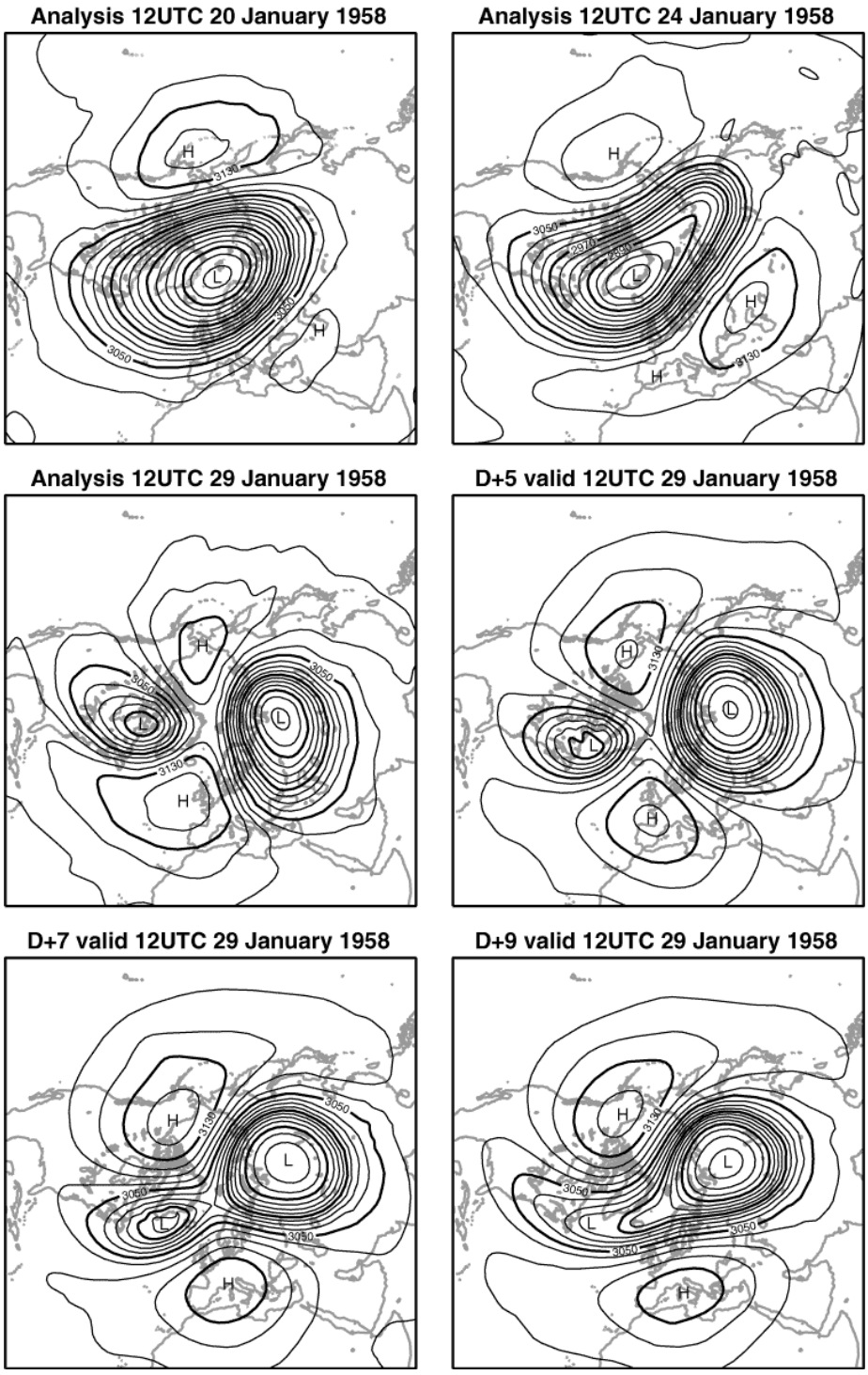

Figure 1 10hPa northern hemisphere ERA-40 height analyses for 12UTC 20, 24 and 29 January 1958 (top left and right, middle left) and 5-, 7- and 9-day forecasts valid 12UTC 29 January 1958 (middle left, bottom left and right). Contour interval: 20dam.

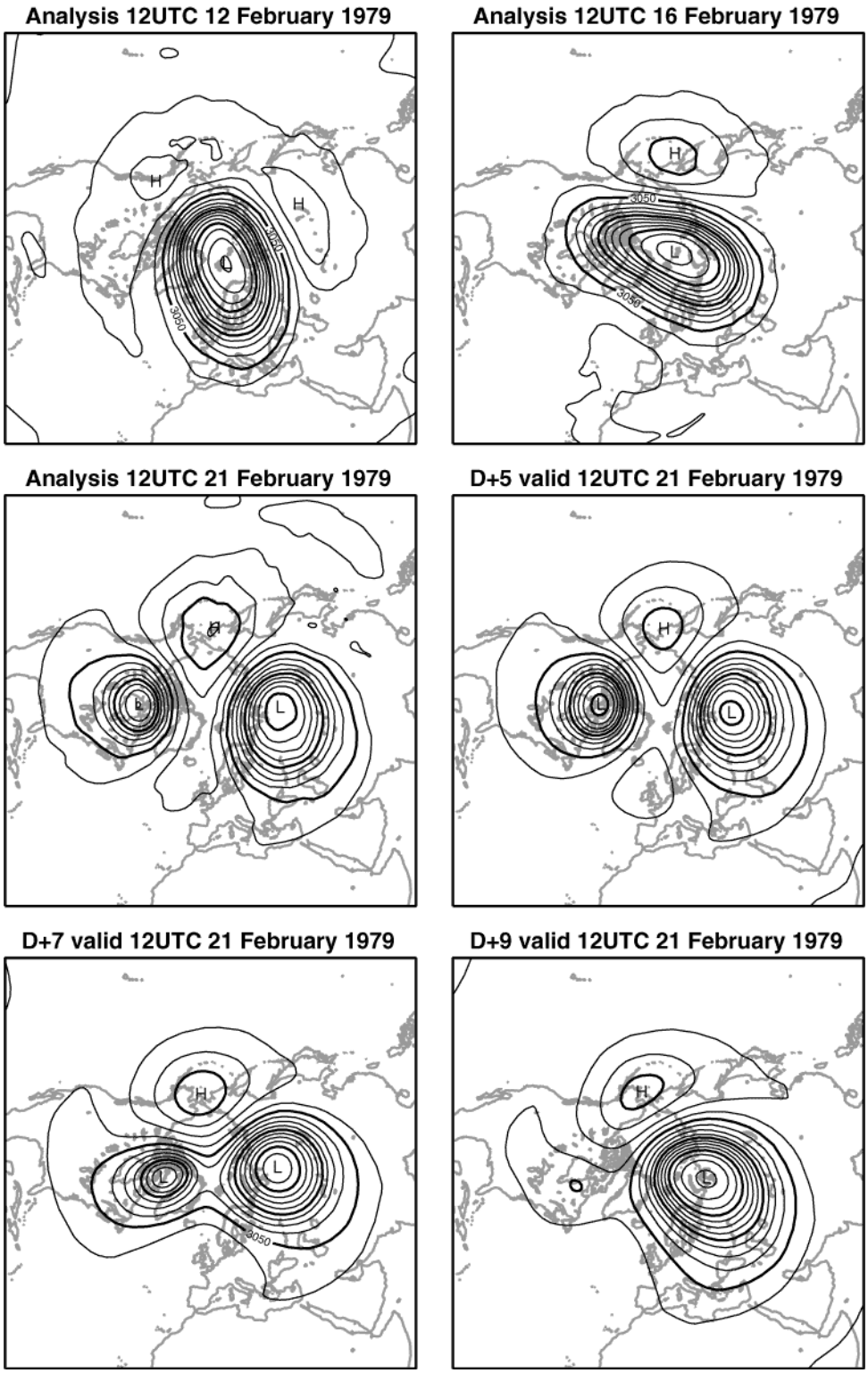

Figure 2 10hPa northern hemisphere ERA-40 height analyses for 12UTC 12, 16 and 21 February 1979 (top left and right, middle left) and 5-, 7- and 9-day forecasts valid 12UTC 21 February 1979 (middle left, bottom left and right). Contour interval: 20dam.

Since then, ECMWF's operational forecasts have proved generally successful at predicting major warming events in the northern hemisphere, for up to a week or so ahead. Figure 3 illustrates operational performance for the most recent case, in February 2003, which resembles that of 1979 in the sequence of 10hPa analysis maps shown. In this instance both five- and seven-day forecasts accurately depict the two cyclonic vortices centred over Canada and Russia and the anticyclone over the Bering Strait. The forecasts are less successful in positioning the weak pressure minimum south of the Aleutian high on 17 February, a more significant feature when viewed in wind maps. Further discussion of this feature is given in section 9.

4 Operational forecasts of the September 2002 event in the southern hemisphere

The stratospheric vortex in the southern hemisphere split completely on 25 September 2002 at 10hPa and above, as depicted in maps of the operational ECMWF analyses of geopotential height.

The top and middle panels of Fig. 4 show the 10hPa height analyses for 15, 20, 25 and 30 September 2002. On the 15th and 20th, the cold vortex was already displaced off the South Pole towards the South Atlantic. An anticyclone was centred south of Western Australia.

Major change occurred over the next five days. The vortex elongated, moved further away from the Pole, and split into two. The anticyclone south of Australia intensified considerably and a smaller anticyclone developed over the South Atlantic. In the course of the following five days, one of the two resulting cyclonic vortices, that over the South Pacific, weakened considerably and moved slightly westward. The other cyclone and dominant anticyclone moved eastward and poleward, the anticyclone continuing to build while the cyclone decayed.

This dramatic evolution of the southern stratospheric circulation was captured extremely well by the ten-day operational forecast made on 20 September. The bottom two panels of Fig. 4 show the five- and ten-day 10hPa height forecasts valid on 25 and 30 September respectively. The five-day forecast is in almost perfect agreement with the analysis. Moreover, the essence of the change from day five to day ten is described, although errors of positioning and intensity do become evident by the end of the forecast range.

Seven- and ten-day operational 10hPa height forecasts valid on 25 September are shown in the left-hand panels of Fig. 5. The seven-day forecast for 25 September is largely successful; at the time illustrated vortex splitting is not quite complete but this is due to a slight delay in timing rather than a failure to capture the split fully. The vortex is unusually elongated, but not split, in the ten-day forecast for this date. Corresponding eight- and nine-day forecasts show the formation of two cyclonic centres, but no complete split of the vortex. Complete vortex splitting occurs at 10hPa in all forecasts made from 18 September onwards, and at 7hPa and above in all forecasts from 17 September onwards.

The right-hand panels of Fig. 5 show the five- and seven-day forecasts valid on 30 September. An improvement can be seen in the location and orientation of the main cyclone and anticyclone from day ten (Fig. 4) to day seven. The remnant of the second cyclone is too weak, and too far to the west over the Pacific at day seven, rather than too far to the east as it is at day ten. This feature is depicted well at the five-day range.

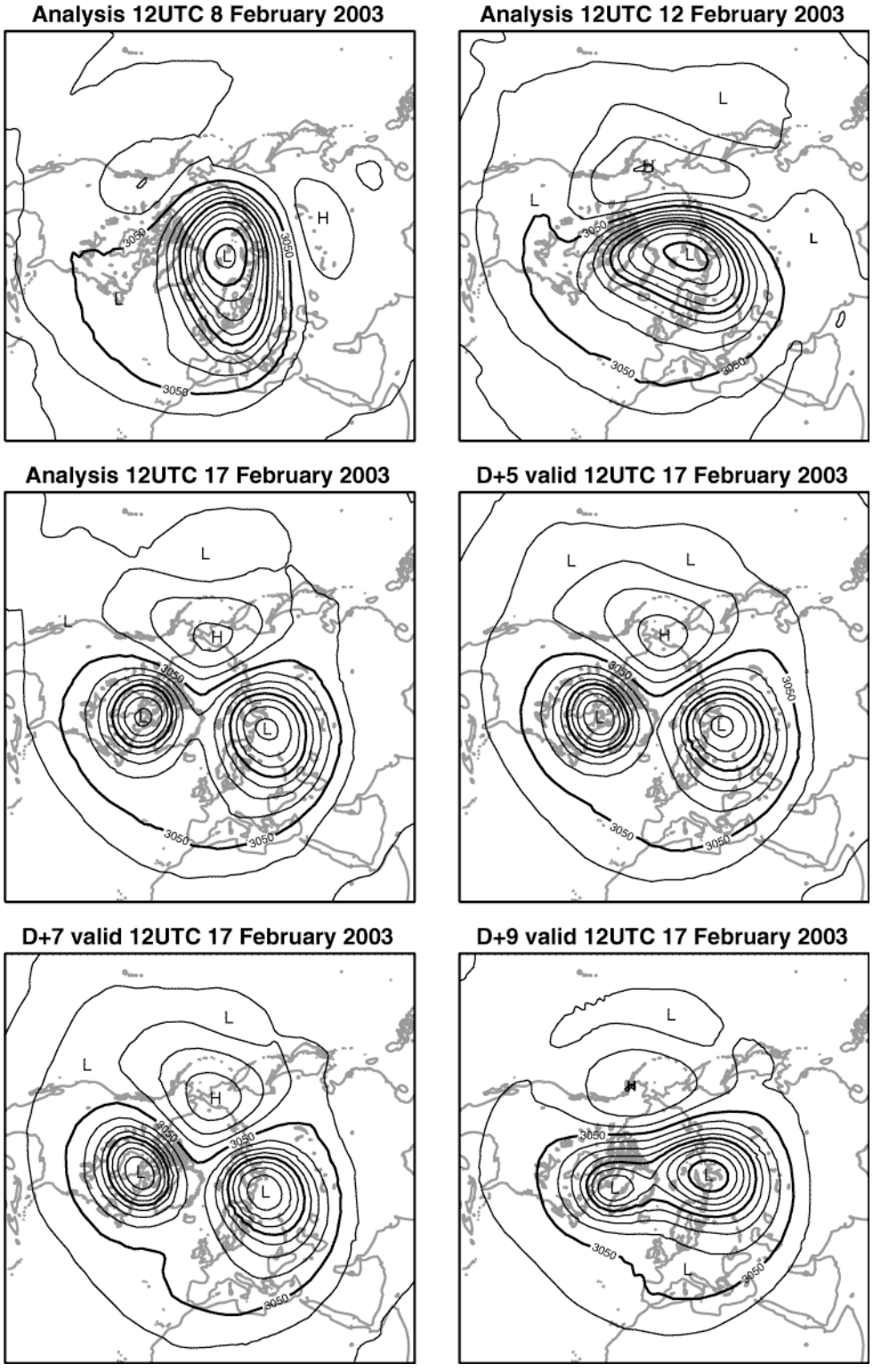

Figure 3 10hPa northern hemisphere operational ECMWF height analyses for 12UTC 8, 12 and 17 February 2003 (top left and right, middle left) and 5-, 7- and 9-day forecasts valid 12UTC 17 February 2003 (middle right, bottom left and right). Contour interval: 20dam.

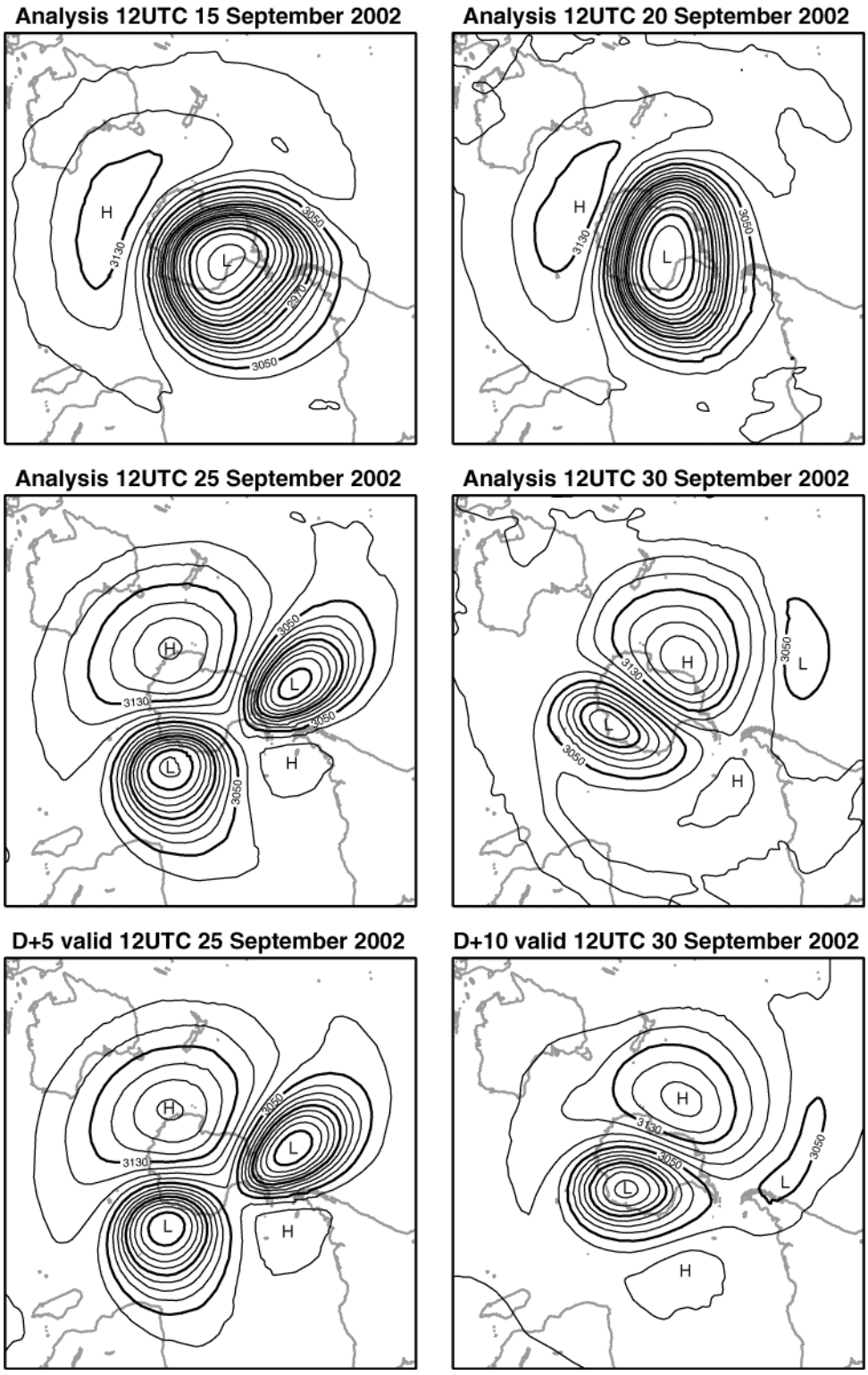

Figure 4 Operational 10 hPa southern hemisphere height analyses for 12UTC 15, 20, 25 and 30 September 2002 (top and middle panels), and 5- and 10-day forecasts from 12UTC 20 September 2002 (bottom panels). Contour interval: 20dam.

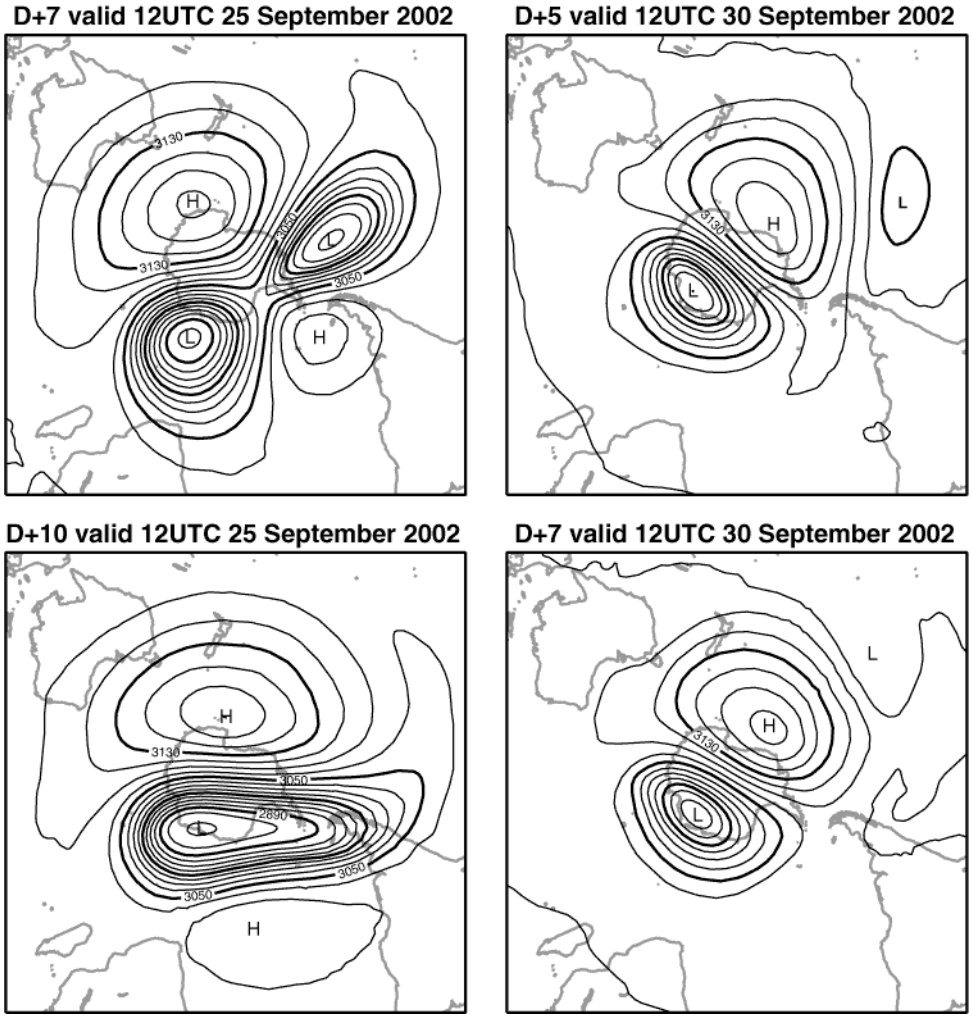

Figure 5 Operational 7- and 10-day 10hPa height forecasts valid 12UTC 25 September 2002 (left) and 5- and 7-day forecasts valid 12UTC 30 September 2002 (right). Contour interval: 20dam.

5 A weak computational instability

The extreme flow conditions in the austral stratosphere in the final week of September 2002 exposed a small-scale computational instability of the forecast model that had not been seen previously in either test or operational use. The instability was self-limiting in that the operational data assimilation and forecast runs did not fail to complete. Nevertheless, considerable localized noise occurred in the analysis for 26 September, and noise was present to a lesser extent on the following day. This can be clearly seen in the 10hPa height analyses for 26 and 27 September shown in the upper panels of Fig. 6. Noise develops in the region of strong easterly flow in each of the two vortices, first appearing close to where the flow lies above mountainous coastal regions of Antarctica. In Fig. 6, the noise has reached large amplitude in part of the Pacific vortex in the operational analysis for the 26th (labelled 25r1) and is present to a lesser extent in the other vortex over and near Queen Maud Land on the 27th. The noise is highly predictable in that it occurs also in forecasts out to as far as eight days ahead valid on these dates, indicating that it is linked to the well-predicted large-scale flow conditions.

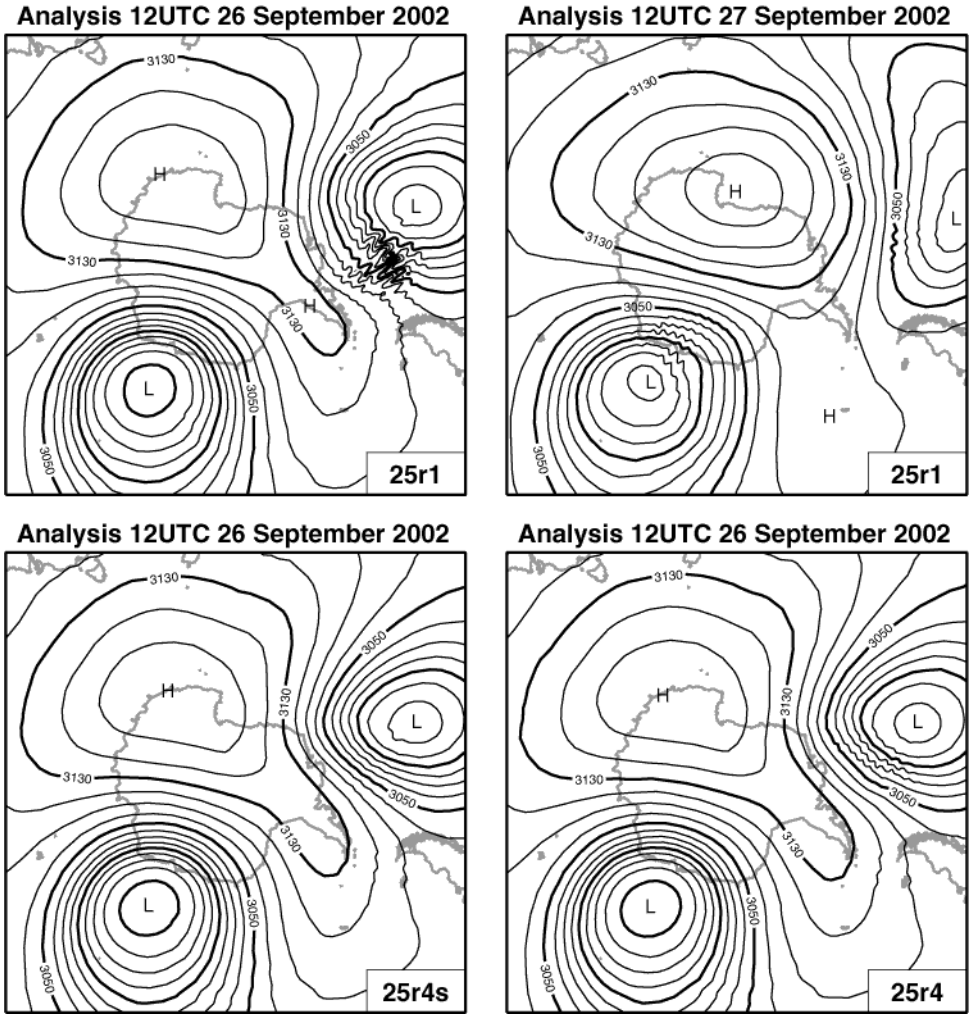

Figure 6 Operational (cycle 25r1) 10hPa height analyses for 12UTC 26 and 27 September 2002 (upper) and rerun analyses for 26 September using cycle 25r4 and either a modified advection scheme (lower left) or a reduced timestep (lower right) in the assimilating model. Contour interval: 20dam.

Linear analysis of the stability of the model's semi-Lagrangian advection scheme (Hortal 2002) shows that the scheme can indeed be unstable if the change in velocity along a single-timestep trajectory is sufficiently large. In the present case the change in the vertical component of the velocity has been found to be the cause of the problem. This appears to be associated with gravity waves generated by flow over the Antarctic coastal mountains. These waves propagate upwards and amplify in the regions of easterly vortex flow. Using a stable, first-order scheme for the vertical part of the trajectory calculation removes the noise, but degrades large-scale forecast accuracy when applied everywhere.

6 High-resolution reruns

Given the rarity of occurrence of the instability discussed above, an acceptable practical solution is to monitor the change in vertical velocity along the trajectory in the stratosphere, and to apply the first-order scheme only where a critical value is exceeded. This solution has been tested in a rerun at operational resolution of the data assimilation and forecasts from 1 September to 15 October 2002. In addition to modification of the advection

scheme, cycle 25r4 of the forecasting system was used for the rerun as it had been tested and shown to be ready for operational implementation. The lower-left panel of Fig. 6 shows an almost completely noise-free 10hPa height analysis for 26 September from this assimilation.

A second rerun of the forecasting system has also been carried out using cycle 25r4 at operational resolution. It covers the period 1 August to 30 September 2002, and assimilated sounder data from the NOAA-17 satellite in addition to the data from NOAA-15 and 16 used operationally and for the first rerun. This second rerun was originally set up to test the three-satellite configuration with the new cycle of the forecasting system and to provide a control experiment for a set of observation-denial experiments, rather than specifically for study of events in the southern stratosphere. In this case the timestep was simply halved in the assimilation cycles beyond 12UTC 25 September to limit the computational instability. The lower-right plot of Fig. 6 shows the analysis for 26 September from this second rerun. Noise is much reduced compared to operations, but not to quite the same extent as found from changing the advection scheme. A similar result is found for the rerun analyses for 27 September (not shown).

Apart from the noise, differences between the operational analyses and the two rerun analyses are generally small, although both reruns can be seen to give slightly higher 10hPa heights in the vicinity of the Antarctic Peninsula in the analyses for 26 September shown in Fig. 6. As would be expected, larger differences are evident at later ranges of the forecasts carried out from these analyses. An example is shown in Fig. 7, which presents five- and ten-day 10hPa height forecasts from the analysis for 20 September 2002 using cycle 25r4 and data from the three NOAA satellites. Comparing with the operational forecasts presented in Fig. 4, there is little difference at five-day range apart from a very slightly earlier split of the vortex in the case of cycle 25r4. The ten-day forecast from cycle 25r4 is, however, clearly superior in this case. More generally, objective verification such as presented in the following section indicates a small but statistically significant benefit from use of cycle 25r4 in the first half of the forecast range, and a very modest additional benefit from use of the additional data from the NOAA-17 satellite. Except where indicated, the results from cycle 25r4 presented in the remainder of this report are based on the longer assimilation carried out using data from the three NOAA satellites, which is the configuration of the ECMWF forecasting system that became operational in January 2003.

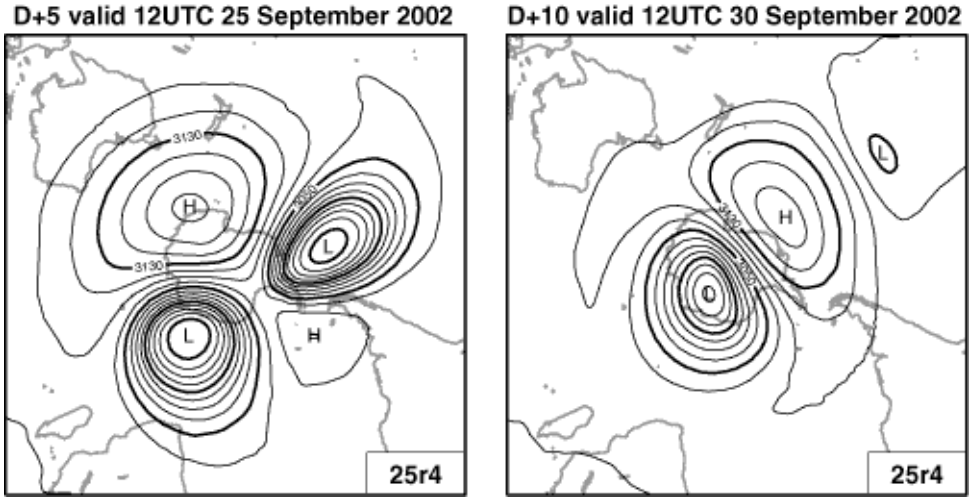

Figure 7 5- and 10-day 10 hPa height forecasts from 12UTC 20 September 2002, produced using cycle 25r4 of the ECMWF forecasting system and assimilating data from three ATOVS satellites. Contour interval: 20dam.

Figs. 8 and 9 present maps of the distributions of potential vorticity and water vapour on the 850K isentropic surface. They complement the maps of 10hPa height already shown. Fig. 8 shows fields derived from the cycle 25r4 rerun analyses for 20 and 25 September 2002, and from the five-day rerun forecast from 20 September. The analysed vortex at this level is characterized not only by large negative values of potential vorticity but also by relatively high values of water vapour. The latter arise from the modelled descent of air moistened by methane oxidation near the stratopause in the background forecasts of the data assimilation. In the ECMWF assimilation system, background stratospheric values of potential vorticity are changed (predominantly on medium to large scales) by analysis increments to the wind and temperature fields, whereas background stratospheric humidity is unchanged by the analysis. Quantitative values of humidity are open to question in the tropics, where representation of the slow upward transfer of dry air above the cold tropopause is not captured as well by the data assimilation as in the free-running simulations reported by Simmons *et al.* (1999). The contrast between a moist polar vortex and dry tropics is nevertheless at least qualitatively realistic, given that temperatures are not cold enough in the vortex to have caused condensation at this level or above.

The principal features of the potential vorticity (PV) and humidity fields are strikingly similar in pattern. Both fields change from day to day primarily due to advection by the distribution of winds on the isentropic surface. Small-scale structure is also introduced directly into PV (but not humidity) by the model's parametrized orographic drag. This in particular modifies PV within the vortex (or vortices) over Antarctica.

Fig. 8 shows clearly the well-predicted split of the vortex already seen in the height-field maps of Fig. 4. It also shows multiple extended streams of large-PV/moist air (darker-shaded bands) extruded from the vortex or vortices, and streams of small-PV/dry air (lighter-shaded bands) drawn in from low latitudes. The maps for 20 September depict in particular a band of air spiralling from low latitudes over the Pacific, across South America and the South Atlantic, towards Antarctica. Such a feature is seen repeatedly in the analyses for August and September. The minimum (in specific humidity and the magnitude of PV) over Queen Mary Land (around 90^{o}E) on 20 September can be traced over the next five days to the location of the centre of the intensified anticyclone south of eastern Australia shown in Fig. 4. Indeed, throughout August and September the growth and movement of anticyclonic features surrounding the vortex in the 10hPa height analyses can be linked with air advected from low latitudes, as identified by distributions of PV and specific humidity on the 850K surface.

Figure 9 shows corresponding analyses and ten-day forecasts for 30 September 2002. There is particularly strong extrusion from both vortices after the split on 25 September, especially from that over the South Pacific, consistent with the weakening of the vortices seen in height fields. Air of recent low-latitude origin almost surrounds each vortex. The ten-day forecasts differ from the analyses in detail, but tell essentially the same story.

The structures seen in Fig. 8 and 9 are dynamically plausible, they indicate basic good behaviour of the model's semi-Lagrangian advection scheme at high horizontal and vertical resolution, and they link with the 10hPa height fields which are generally well analysed. It would nevertheless be of interest to seek such verification of smaller-scale features as is possible using independent satellite data. In this context, the ozone fields produced routinely by the ECMWF system are further candidates for study. The ozone analyses exhibit the principal features on the 850K surface shown for PV and specific humidity in Fig. 8 and 9, but small-scale structure is less evident, due presumably to a stronger effect of source/sink terms in the assimilating model. Maps of total ozone depict the vortex split, but ozone-hole depths are underestimated by some 50 Dobson units compared with retrievals from GOME and TOMS data. Successful forecasts by KNMI of the split of the

ozone hole using a chemical transport model forced by ECMWF's operational meteorological fields have been reported by Eskes (personal communication; ESA news report, 23 September 2002, http://www.esa.int/export/esaCP).

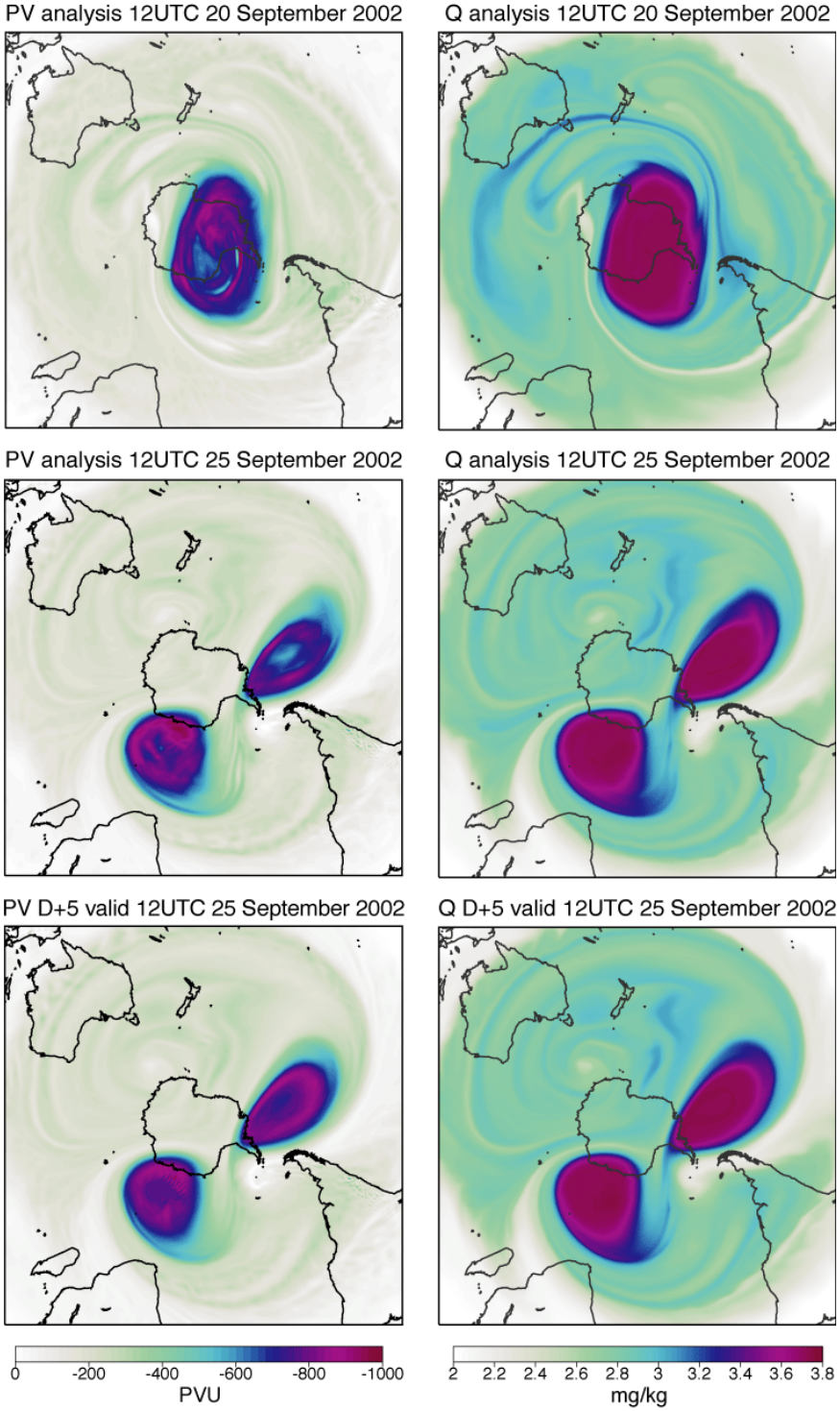

Figure 8 Analyses of potential vorticity (left) and specific humidity (right) on the 850K isentropic surface for 12UTC 20 and 25 September 2002 (top and middle), and corresponding 5-day forecasts valid 25 September 2002 (bottom). Shading is from 0 to -1000 PVU for potential vorticity (1PVU=$10^{-6}m^2s^{-1}Kkg^{-1}$) and from 2 to 3.8 mg/kg for specific humidity.

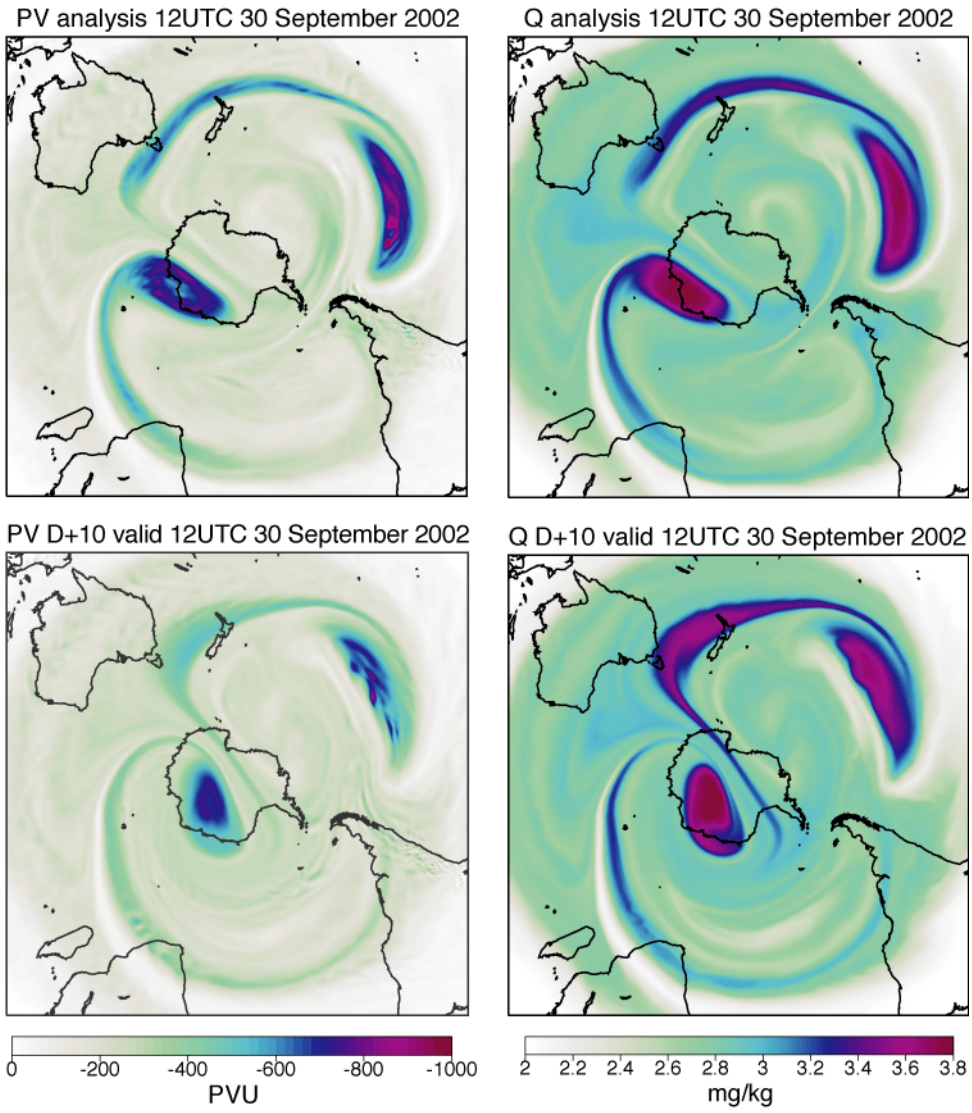

Figure 9 Analyses of potential vorticity (left) and specific humidity (right) on the 850K isentropic surface for 12UTC 30 September 2002 (upper), and corresponding 10-day forecasts valid at this time (lower). Shading is from 0 to -1000 PVU for potential vorticity and from 2 to 3.8 mg/kg for specific humidity.

It is beyond the scope of this report to investigate either the mechanism of the vortex split itself or the origin of the unusual conditions that led to its occurrence in 2002. The analyses produced by ECMWF and other NWP centres are nevertheless important resources for such investigations. Future studies that are to be based on ECMWF data should use the improved rerun analyses discussed here in preference to the corresponding operational analyses. Access details are specified in the Appendix.

7 Analysis and forecast accuracy

In this section we examine further the accuracy of the cycle 25r4 results for August and September 2002 in the austral middle stratosphere.

Fig. 10 presents time series of radiosonde observations of 20hPa temperature from three stations located near the Antarctic coast, together with corresponding time series of analysed and forecast values at the three

locations. The forecast start times are 12UTC, and the ranges are 4.5 or 5 days (referred to as D+5) and 9.5 or 10 days (referred to as D+10), depending whether the verifying observations are for 00 or 12UTC[1]. 20hPa is the level of maximum analysed warming over the six days beginning 12UTC 20 September and is a standard reporting level reached by a reasonable number of radiosonde ascents. The locations of the three stations, Casey, Syowa and Halley, are indicated by the labelled observations plotted on the left-hand map in Fig. 11.

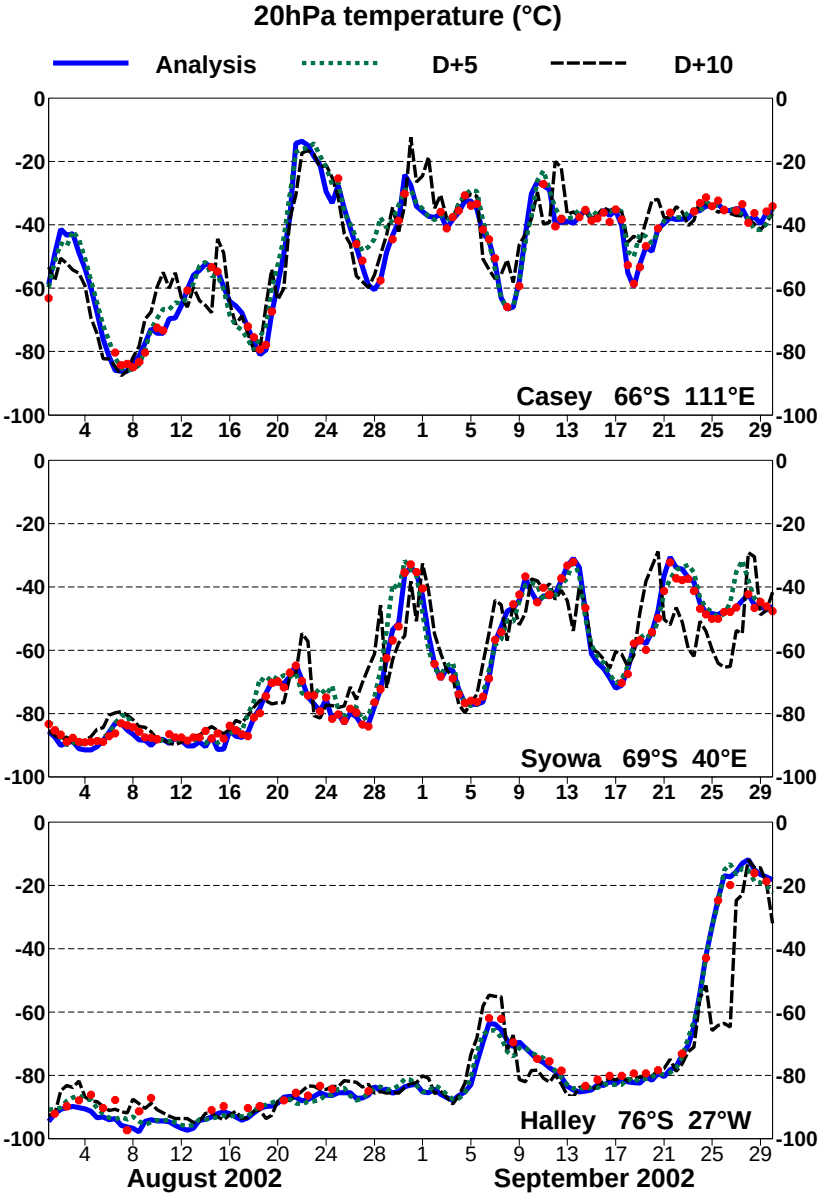

Figure 10 Time series of 20hPa temperature (^{o}C) for August and September 2002 at the locations of three Antarctic radiosonde stations: Casey (66^{o}S,111^{o}E, top panel), Syowa (69^{o}S,40^{o}E, middle panel) and Halley (76^{o}S,27^{o}W, bottom panel). Solid red circles denote radiosonde measurements and the blue solid lines denote analyses. Values for 00 and 12UTC are plotted. Green dotted lines (labelled D+5) denote 108- and 120-hour forecasts valid at these times (started from 12UTC initial analyses), and black dashed lines (labelled D+10) denote corresponding 228- and 240-hour forecasts. Results are from cycle 25r4, with NOAA-17 data assimilated in addition to data from NOAA-15 and 16 except for the forecasts with start dates prior to 1 August.

1. The times given in radiosonde reports vary from station to station. Reports timed at either 23UTC the previous day or 00UTC are regarded here as observations for 00UTC, and 11UTC and 12UTC reports are likewise both regarded as observations for 12UTC.

Fig. 10 shows large oscillations in temperature at Casey (66°S, 111°E) in August and early September, associated with distortion and movement of the vortex, whose cold core lies over the station at some times but not at others. For most of the rest of September the vortex no longer overlies the station, as can be seen for the sample days for which analyses have been presented in Figs. 4 and 8. Temperatures in this later period are reported to be mostly a little above -40°C. The observations at Syowa (69°S, 40°E) reveal cold temperatures between about -90°C and -80°C in the first half of August. Temperatures at this station subsequently fluctuate as the soundings become influenced by vortex changes in the period up until the last ten days of September. Cold air (with temperatures mostly below -80°C and reaching as low as -97°C) lies above Halley (76°S, 27°W) until the end of September, when the observations (which are for 12UTC) show a rapid temperature rise of almost 60°C over the six days from 20 to 26 September as the vortex splits. A map of the differences between the analyses for these two days reveals a warming that reaches a maximum of 84°C at 70°S 67°W over the Antarctic Peninsula.

The analysed values shown in Fig. 10 fit the radiosonde observations very closely, as do the forecasts at the D+5 range, with just a few exceptions. Indeed, the major oscillations are captured quite well even at the D+10 range. The largest discrepancy is at Halley, where the ten-day forecasts from 15 and 16 September fail to indicate the strong warming associated with the vortex split. Fig. 10 provides an indication that high levels of forecast skill are not unique to the late-September period.

Snapshots for 25 September indicating good fit to observations are presented in Figs. 11 and 12. Fig. 11 shows contour maps of the 12UTC 20hPa temperature analysis and the five-day forecast for this time, with the available radiosonde measurements superposed. A remarkable agreement is again seen between the analysis and the five-day forecast. Both analysis and forecast match well the measurements from the limited number of radiosonde ascents. The temperature shown for Halley is 54°C warmer than the corresponding measurement at the initial time of the forecast.

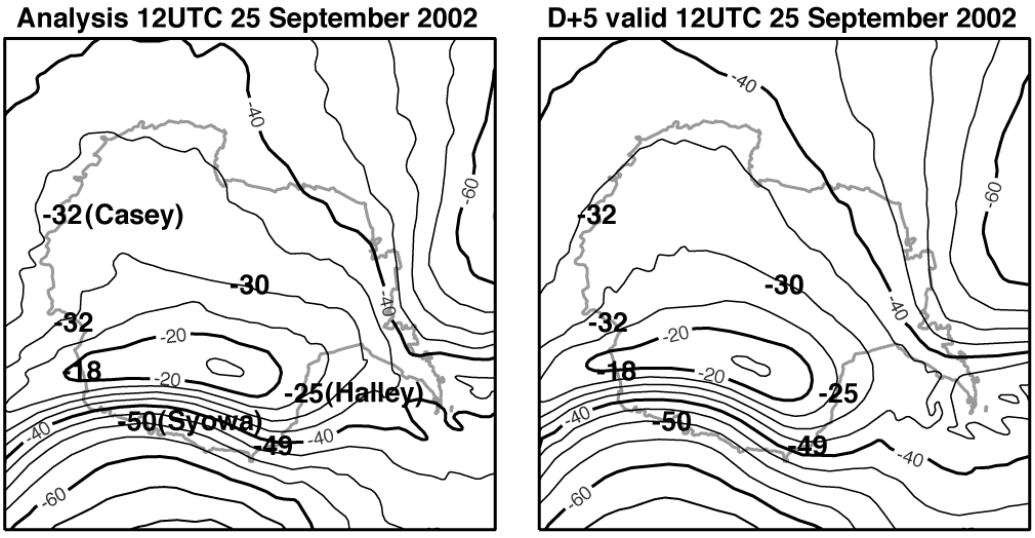

Figure 11 20 hPa temperature analysis (left) and 5-day forecast (right) valid 12UTC 25 September 2002 (contour interval: 5°C). The heavier black numbers are corresponding radiosonde measurements of 20hPa temperature. Those from the Antarctic coastline stations are for report times of 11 or 12UTC. A measurement from the South Pole station is not available for either of these times; the average of the 00UTC reports for 25 and 26 September is plotted instead for this station.

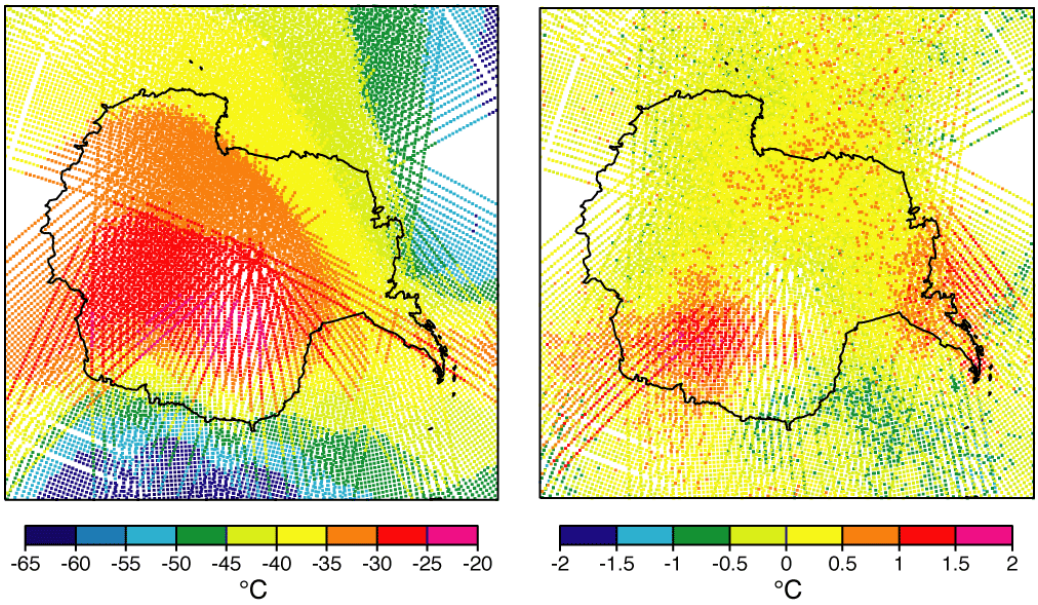

Figure 12 AMSU-A channel-11 brightness temperatures (°C) from the NOAA-16 and NOAA-17 satellites for the 4D-Var assimilation window 03-15UTC 25 September 2002 (left) and corresponding differences (right) from simulated brightness temperatures derived from model background fields.

A much denser observational coverage is provided by the soundings from polar-orbiting satellites. The left-hand panel of Fig. 12 shows radiance measurements from channel 11 of the AMSU-A instruments on NOAA-16 and NOAA-17, accumulated over the assimilation period 03-15UTC on 25 September. Channel 11 ceased working on NOAA-15 earlier in 2002, but data from adjacent channels were available and assimilated for the period in question, providing coverage over the two blank triangular regions in Fig. 12 where no channel-ll measurement is available. The radiance measured by channel 11 is most sensitive to the atmospheric temperature at about 20hPa, although it is influenced by values over a deep stratospheric layer, temperatures at 50 and 10hPa having half the influence of temperature at 20hPa. The distribution of channel-11 brightness temperatures is nevertheless in quite close agreement with the 20hPa temperature analysis shown in Fig. 11.

The right-hand panel of Fig. 12 shows corresponding differences between the measured radiances and radiances simulated using the 4D-Var background forecast from 00UTC 25 September. These differences generate a 12UTC analysis increment due to the channel-11 data. The differences are small, less than 1°C in brightness temperature at most points. Red-coloured spots show where the measured radiances are most in excess of the simulated radiances. The channel-11 data tend to warm the analysis (or equivalently correct a slightly cold background field) west of the Antarctic Peninsula and over and to the east of Queen Maud Land.

A selection of analysis and forecast verification statistics is presented in Fig. 13. Root-mean-square errors of 20hPa temperature and vector wind are shown, evaluated over the extratropical southern hemisphere and averaged for initial analyses and forecasts run from 12UTC daily for the period 1 August to 30 September 2002.

The top panels of Fig. 13 show verification of cycle 25r4 forecasts against subsequent cycle 25r4 analyses for 00 and 12 UTC, and verification of the same forecasts and of the initial analyses against radiosonde measurements for these times. A diurnal cycle in the verification against radiosondes is due to a difference in the geographical distribution of the verifying observations at 00 and 12UTC. If forecast error is not uniformly distributed over the extratropics, it is sampled differently by the radiosondes at the two verification times.

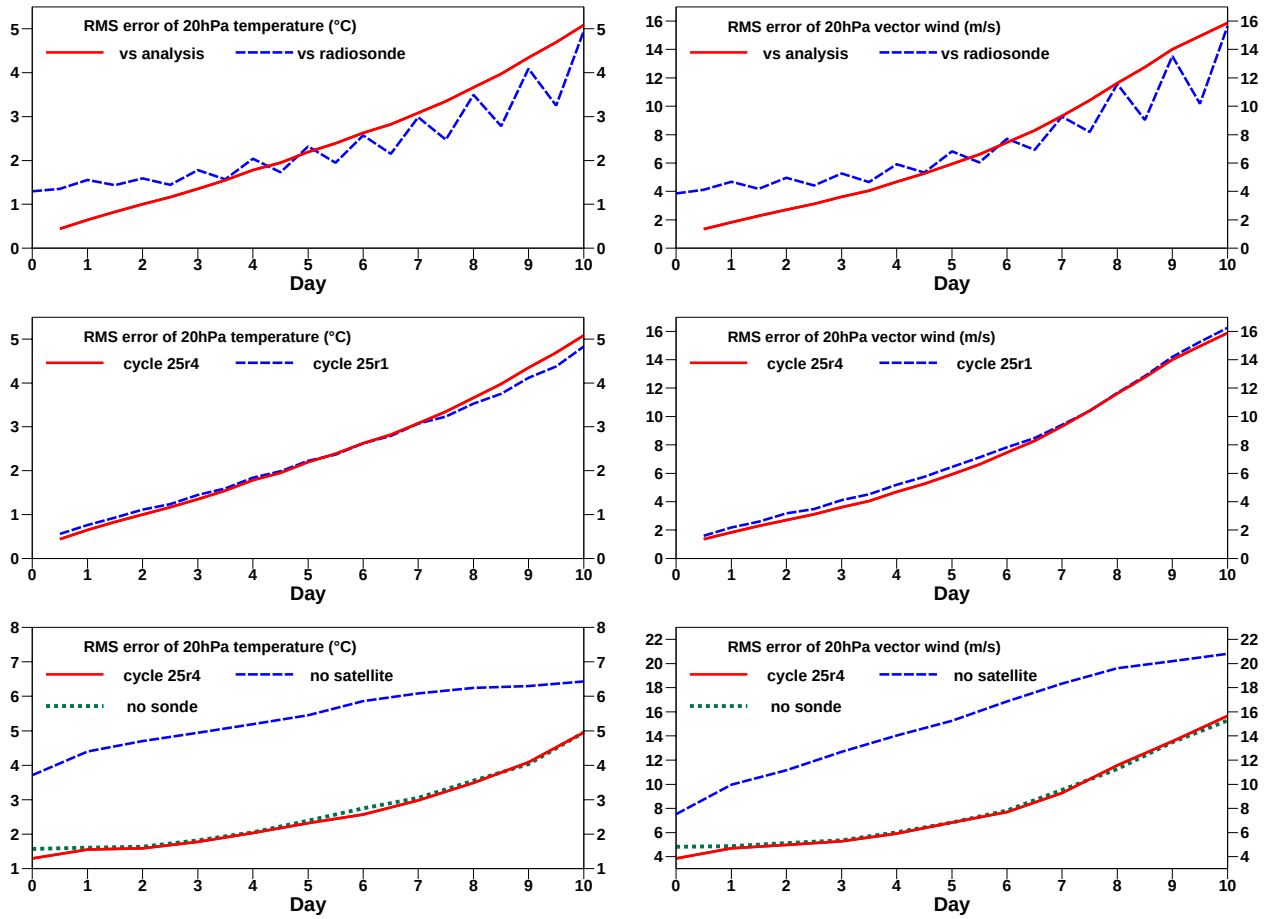

Figure 13 Root-mean-square errors of 20hPa temperature (^{o}C, left) and of vector wind (ms^{-1}, right) for the extratropical southern hemisphere, averaged over forecasts carried out from 12UTC for each day of August and September 2002. The top panels show verification of cycle 25r4 forecasts against analyses (also from cycle 25r4; red solid lines) and against radiosonde data (blue dashed lines) at 00UTC and 12UTC. The middle panels show errors of forecasts from cycles 25r4 (red solid lines) and 25r1 (blue dashed lines) verified against corresponding analyses. The bottom panels show errors of standard cycle 25r4 forecasts (red solid lines) and of corresponding forecasts from analyses in which satellite data were withheld (green dotted lines) and in which radiosonde, pilot-balloon and wind-profiler data were withheld (blue dashed lines), for verification against radiosonde data (at 12UTC only).

Verification against analyses indicates lower forecast errors than verification against radiosondes out to about five days ahead. The verification against radiosondes exhibits slow error growth and little diurnal variation over this part of the forecast range. Corresponding mean errors against radiosondes (not shown) are of the order of 0.5^{o}C for temperature and 1ms^{-1} for wind. These results suggest that initial analysis errors and consequential short-range forecast errors are much smaller than the errors of the verifying radiosonde observations. In this context, radiosonde observation errors comprise not only direct measurement errors, but also errors of timing and location (the whole balloon-based sounding is assumed valid at the single reported time and location) and representivity (if the measurement is influenced by small-scale motion unresolved in analyses and forecasts). The implied random analysis errors are of the order of a few tenths of a degree in temperature and 1ms^{-1} in wind. The corresponding values for five-day forecast errors are about 2^{o}C and 6ms^{-1}. The small implied analysis errors for temperature are consistent with the accuracy of fit of simulated and measured AMSU-A brightness temperatures. The implied radiosonde observation errors of 1^{o}C or a little more for temperature and about 4ms^{-1} for wind at 20hPa are reasonably consistent with the corresponding values of 1.5^{o}C and 3.3ms^{-1}

specified in the data-assimilation system. The specified observation error for the AMSU-A channel-11 brightness temperature is 0.35^{o}C.

Quite similar analysis, forecast and radiosonde-observation errors are inferred from corresponding verifications for the 30, 50 and 70hPa levels.

The middle panels of Fig. 13 show verifications against analyses comparing the cycle 25r4 forecasts with the operational (cycle 25r1) forecasts. The improvement of cycle 25r4 over cycle 25r1 out to five days ahead (rather larger for wind than temperature) is statistically significant, at the 0.1% confidence level for a t-test applied to the wind-score differences, assuming them to be temporally uncorrelated. The superiority of the newer cycle is clearly confirmed by verification against radiosondes in the case of the wind field (not shown). This supports the recommended use of the high-resolution rerun analyses rather than the operational analyses for further studies. The poorer temperature scores for cycle 25r4 beyond day seven are of low statistical significance.

The bottom panels of Fig. 13 show verifications against 12UTC radiosondes of the standard 25r4 forecasts and of forecasts from assimilations in which either all satellite data or all radiosonde data[1] were withheld throughout the August and September period. Withdrawing radiosonde data from the assimilation not surprisingly results in analyses which do not fit the radiosonde data as well, as shown by the day-0 differences in the plots. There is, however, almost no degradation of subsequent forecast quality from this data denial. Five- and ten-day 10hPa height forecasts run from the no-radiosonde analysis for 12UTC 20 September are shown in Fig. 14 and can be seen to be similar to the cycle 25r4 control forecasts shown in Fig. 7.

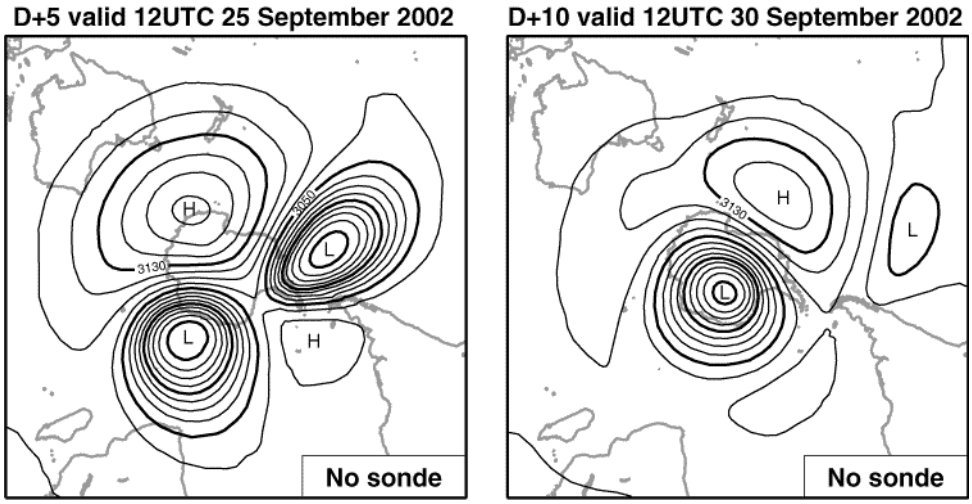

Figure 14 5-day (left) and 10-day (right) forecasts for 12UTC 25 and 30 September 2002 respectively from an assimilation in which radiosonde, pilot-balloon and wind-profiler data were withheld. Contour interval: 20dam.

In contrast, removing the satellite data causes a very substantial degradation of the fit of analyses and forecasts to the radiosonde data. The analysis for 25 September (not shown) represents quite well the strong anticyclone south of eastern Australia, but produces a vortex that is unusually elongated rather than split,

1. Pilot-balloon and wind-profiler data were also withheld in what for simplicity we refer to as the assimilation without radiosonde data. Moreover, the bias corrections that were applied to the satellite data used in this assimilation were derived from earlier assimilations that used radiosonde data (Harris and Kelly, 2001).

similar to that displayed in Fig. 5 for the ten-day operational forecast valid for this day. It should be stressed that the no-satellite assimilation used the same background error statistics as the standard cycle 25r4 assimilation. A better use of the limited available radiosonde data could have been made by specifying larger background errors (as was done to a degree for the ERA-40 system). The present results nevertheless demonstrate the overwhelming role played by satellite data in determining the high quality of analyses and forecasts for the southern-hemisphere stratosphere produced by the current ECMWF forecasting system.

8 A search through the ERA-40 archives

When the southern hemisphere vortex broke up in September 2002 it was thought to be an event that had never before been observed. For confirmation, 10hPa height analyses from ERA-40 have been examined for each day in September and October from 1957 to 2001.

No instance of pronounced vortex splitting similar to that of 2002 has been found. It is not uncommon to see a marked weakening of the vortex towards the end of October, and the weakening vortex may be displaced from the pole as a prelude to the establishment of summertime easterlies. This commonly occurs in conjunction with formation of a relatively strong anticyclone in the Australian sector, with the vortex displaced into the Atlantic/American sector, as indeed occurred prior to the vortex split in September 2002. This displacement tends to keep cold air over the Halley radiosonde station. This suggested examining all 20hPa radiosonde temperature observations from Halley processed by ERA-40 for the months of September and October from 1957 onwards to see how unusual were the warm temperatures reported at Halley in late September 2002. No observation was found that was warmer than the value of -16^{o}C measured in the ascent from Halley on 28 September 2002, the maximum value shown in the time series presented in Fig. 10.

20hPa temperature reports from all other Antarctic stations located poleward of 70^{o}S have also been examined for the months of September and October from 1957 to 2002. The warmest temperature in 2002 was $-10\,^{\circ}\mathrm{C}$ measured at Neumayer (71^{o}S, 8^{o}W), also on 28 September. This is higher than any earlier 20hPa temperature in the ERA-40 database for this set of stations and the two months in question. The previous high values of $-11\,^{\circ}\mathrm{C}$ from Vostok (78^{o}S, 107^{o}E) on 14 October 1979 and $-12\,^{\circ}\mathrm{C}$ from the South Pole on 28 October 2000 were each associated with displacement of the (single) analysed vortex away from the pole into the Atlantic/American sector. Fig. 15 shows 20hPa temperature analyses and radiosonde measurements over Antarctica, and 10hPa height analyses over a larger southern hemisphere domain, for the three dates concerned.

Comment must be made on biases in south-polar stratospheric temperatures in the ERA-40 analyses. Mean temperatures for late winter and early spring for the pre-1973 period, when no satellite data and only particularly sparse radiosonde data were assimilated in the stratosphere, are typically colder than those for later years by 10^{o}C or more south of 60^{o}S between 20 and 50hPa. A similar bias was reported by Simmons *et al.*(1999) for an earlier version of the model run in climate-simulation mode. The early analyses are thus liable to overestimate the intensity of the austral polar vortex and may not provide a reliable representation of perturbations to it. Temperature biases are smaller when satellite data are assimilated, but the later ERA-40 analyses exhibit an oscillatory temperature structure in the vertical with an amplitude of a few degrees throughout the Antarctic stratosphere that is seen neither in other climatologies (Randel *et. al.*, 2002) nor in recent operational analyses. Biases against southern-hemisphere radiosonde observations are correspondingly much larger than in recent operations. A problem in the 3D-Var assimilation of radiance data in ERA-40 that is not experienced in the operational 4D-Var system is the likely cause. This has little impact on analysed synoptic characteristics, which are very similar in ERA-40 and operations for the 1999-2001 period when

both assimilations used similar vertical resolution in the stratosphere. It nevertheless complicates the interpretation of time series of analysed Antarctic temperatures.

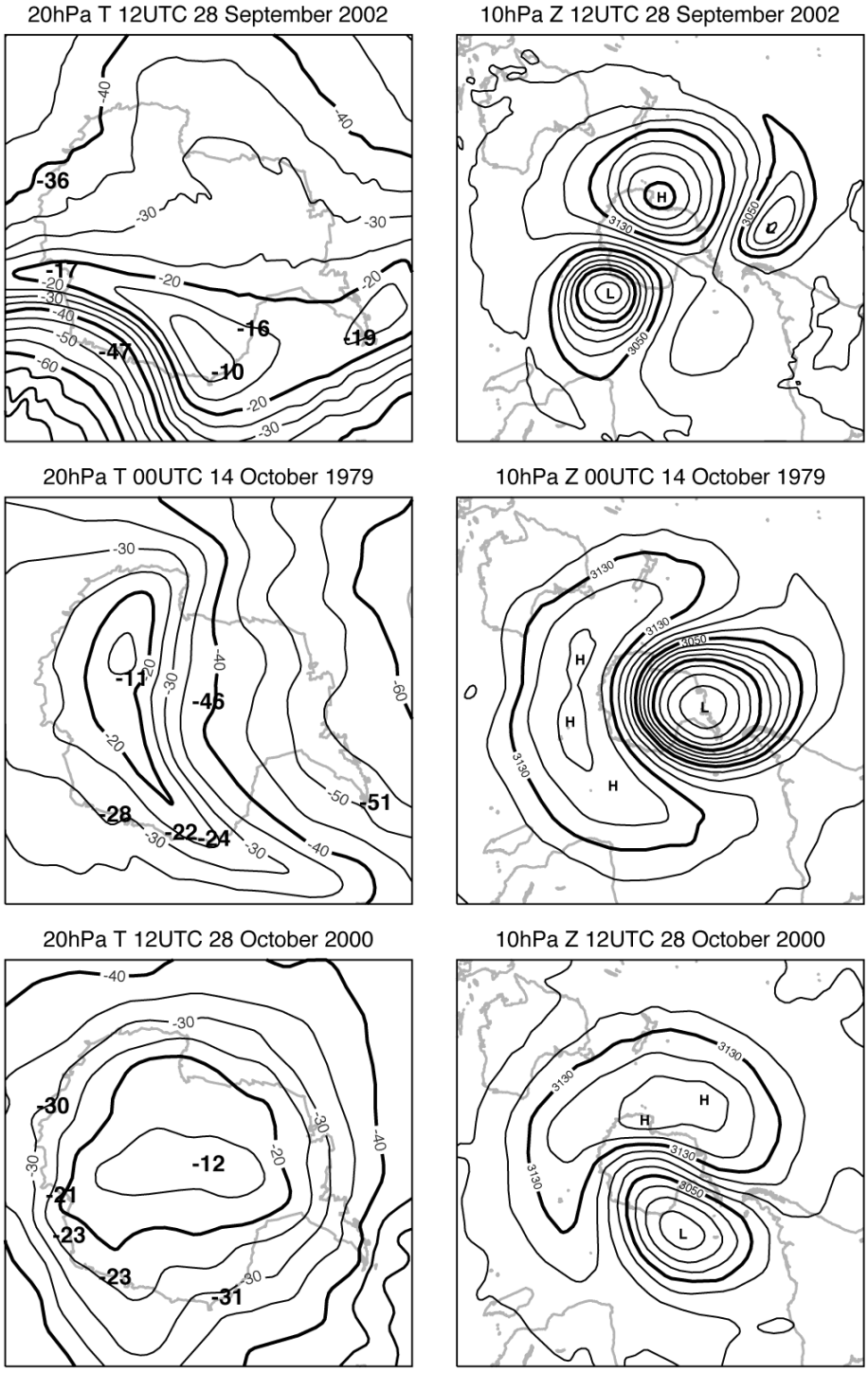

Figure 15 Analyses of 20hPa temperature (left) and 10hPa height (right) from the cycle 25r4 rerun for 12UTC 28 September 2002 (top) and from ERA-40 for 00UTC 14 October 1979 (middle) and 12UTC 28 October 2000 (bottom). 20hPa radiosonde temperature measurements are plotted as heavier black numbers on the left-hand maps. Contour intervals: 5°C and 20dam.

9 Secondary vortex development

Searching through the ERA-40 archives did reveal a number of cases in which the analysed vortex elongates considerably and distorts, but does not break-up into two vortices of similar intensity. One such case, shown in Fig. 16, was found for 29 October 1972, when the 20hPa temperature measurement from Halley reached -19^{o}C, the highest September or October value from this station prior to September 2002, according to the ERA-40 database. The analysis in this case must be viewed with caution, however, as only very limited amounts of stratospheric radiosonde data from Antarctic stations were available for assimilation, on average about two reports per day at 20hPa, three at 30hPa and five at 50hPa in the week leading up to 29 October.

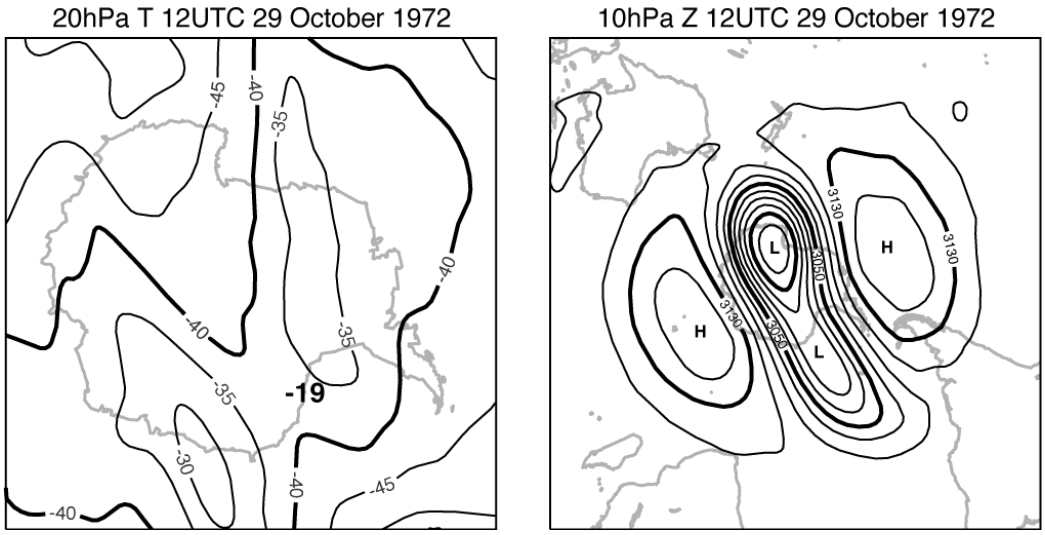

Figure 16 ERA-40 analyses of 20hPa temperature (left) and 10hPa height (right) for 12UTC 29 October 1972. The only available 20hPa radiosonde temperature measurement is plotted as the heavier black number on the left-hand map. Contour intervals: 5^{o}C and 20dam.

Fig. 17 presents a more recent example based on better data coverage, which serves also to illustrate additional diversity in vortex dynamics. The figure shows maps of 10hPa height and 850K PV and specific humidity for 21, 23 and 25 October 1994. On 21 October the vortex is highly elongated and bowed, and flanked by two anticyclones. The height map for two days later shows a second low centre in the main vortex, but this does not develop further. There is also a weak low-pressure centre cut-off from the trailing portion of the main vortex, located west of South America. This cut-off low subsequently moves westward around the Pacific anticyclone and intensifies. The PV and humidity maps for 25 October each depict cyclonic wrapping up near the end of a band of material extruded from the main vortex. The picture is somewhat sharper for humidity, which is a prognostic model grid-point variable, than for PV, which is derived from the model's spectrally-represented prognostic dynamical variables. The left-hand panel of Fig. 18 presents a local map showing the distributions of Montgomery potential and wind for the developing perturbation on the 850K isentropic surface. The tilt of the system is counter to the shear of the ambient flow, indicating that barotropic instability of the local easterly flow around the Pacific anticyclone plays a role in the intensification.

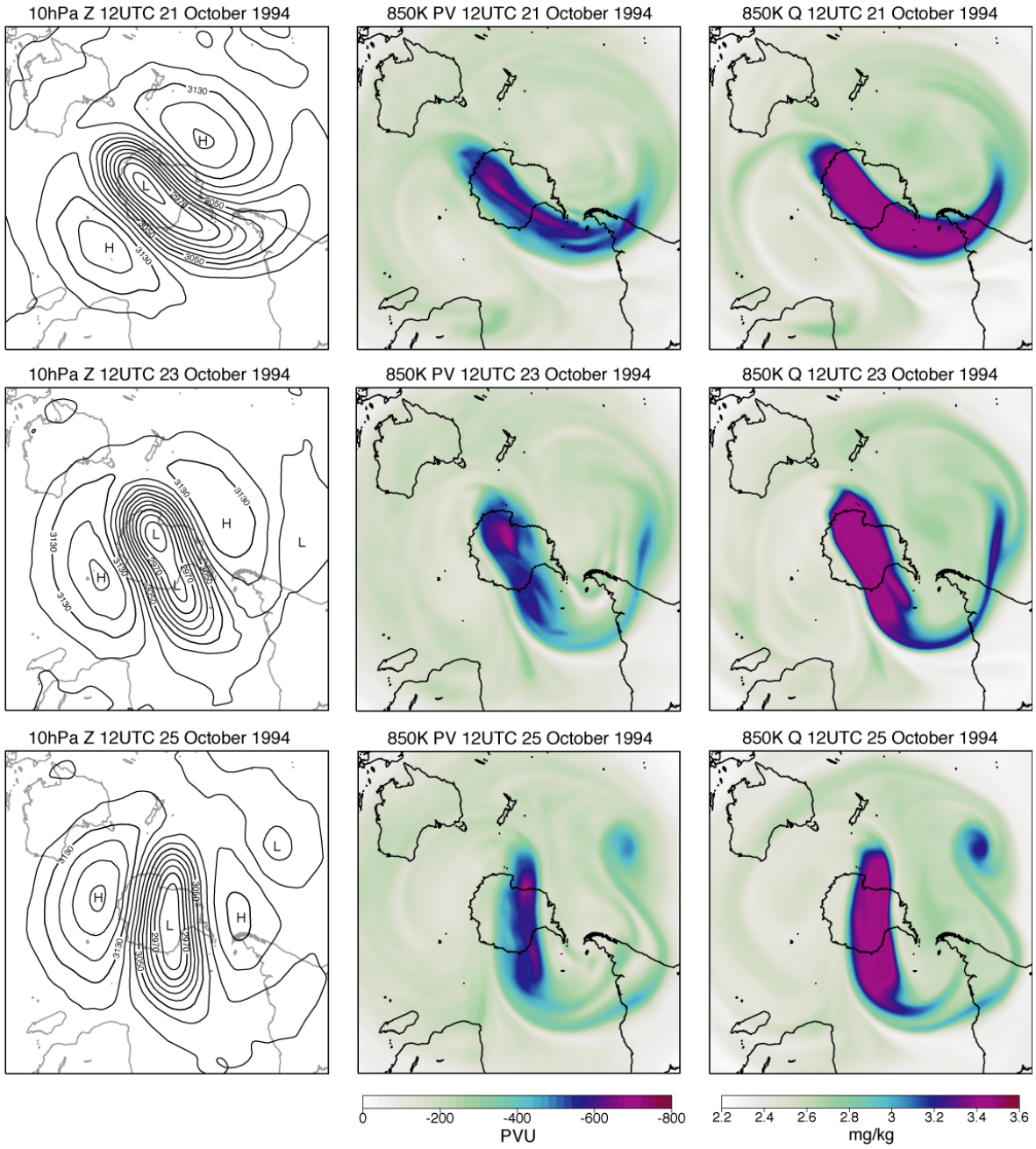

Figure 17 ERA-40 analyses of 10hPa height (left) and 850K potential vorticity (centre) and specific humidity (right) for 12UTC 21, 23 and 25 October 1994. The contour interval for height is 20dam, and shading is from 0 to -800 PVU for potential vorticity and from 2.2 mg/kg to 3.6 mg/kg for specific humidity.

Hartmann *et al.*(1996) indicated the possibility of such perturbation growth by applying a singular-vector analysis to a case of extrusion of high-PV air around the Aleutian anticyclone in the wintertime northern hemisphere. An example of this is provided by the weak low near the dateline in the analysis for 17 February 2003 shown in Fig. 3. The right-hand panel of Fig. 18 shows it to have a structure in its developing phase that is very similar to that of the October 1994 case (taking into account the basic hemispheric difference).

The same process also appears to be responsible for break-up of the extrusion from the weaker of the two southern hemisphere vortices at the beginning of October 2002, following the vortex split one week earlier. Fig. 19 displays contour maps of 10hPa height superimposed on the distributions of specific humidity on the 850K surface for 12UTC on 2 and 4 October 2002. These analyses are from the cycle 25r4 assimilation with modified advection scheme. The figure shows how the original Pacific vortex and band of air extruded downstream of it (depicted in Fig. 9 for 30 September) develops into three synoptic-scale vortices, as features move westward around the strong anticyclone. The map for 2 October also shows a streamer of relatively moist air that is drawn poleward from just south of Australia and wrapped around the primary vortex. This air was extruded from the weaker Pacific vortex several days earlier.

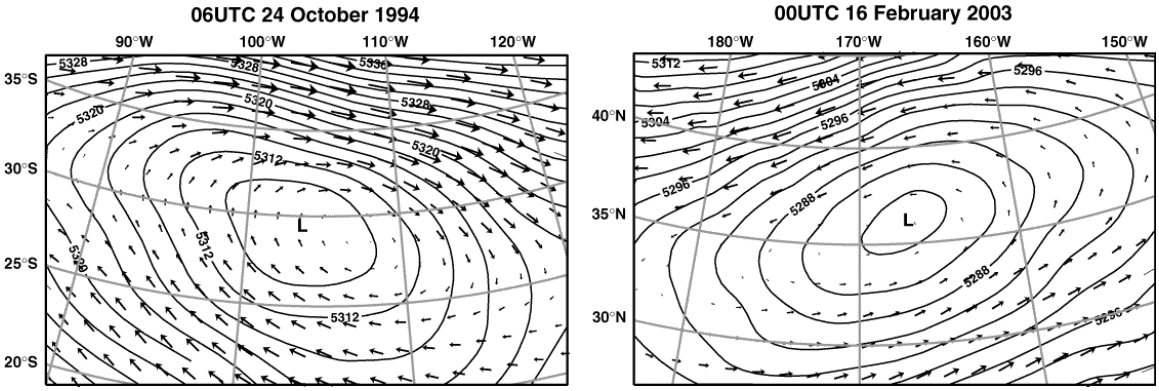

Figure 18 Analyses of 850K Montgomery potential (contour interval 200m^2s^{-2}; contour labels in units of 100m^2s^{-2}) and wind for 06 UTC 24 October 1994 from ERA-40 over the South Pacific (left) and for 00UTC 16 February 2003 from operations over the North Pacific (right). Maximum wind speeds over the areas shown are a little over 40ms^{-1} for the left-hand panel and 30ms^{-1} for the right-hand panel.

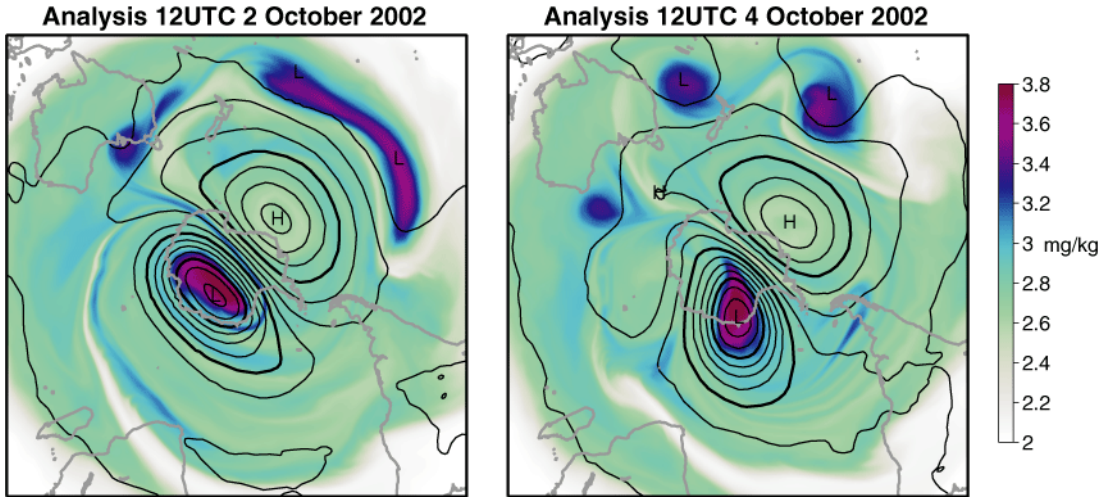

Figure 19 Analyses of 10hPa height (contour interval: 20 dam) and 850K specific humidity (shading from 2.0 to 3.8 mg/kg) for 12 UTC 2 and 4 October 2002.

Comparisons with observations are needed to validate analyses of secondary vortex developments such as discussed above. These developments tend to take place over regions with particularly sparse coverage by *in-*

situ measurements, especially at the heights in question, and are likely to be less well treated by the assimilating forecast model than are forced planetary-scale features. The analysed synoptic-scale systems illustrated for early October 2002 have too shallow a vertical structure for them to be resolved well by AMSU-A measurements, but they move over a region of relatively good *in-situ* data coverage. The data assimilation for this period fits well the 10hPa temperature and wind measurements from Australian and neighbouring radiosondes. In contrast, the secondary vortex near the dateline on 17 February 2003 is a relatively deep feature that increases in intensity above 10hPa and can therefore be "seen" by satellite soundings. Its thermal pattern closely matches the pattern in the assimilated radiances from the high-sounding AMSU-A channels.

Features in analyses that are directly forced at small scales by the assimilating model must be viewed with caution. The PV map for 23 October 1994 presented in Fig. 17 shows U-shaped bands of low and high PV extending from the Antarctic Peninsula into the South Atlantic and then across southern South America and into the Pacific. These bands arise from advection of vorticity forced persistently in a dipole pattern over the Antarctic Peninsula on 22 and 23 October by the model's parametrization of gravity-wave drag. No such feature occurs in the corresponding humidity field. The bands spread to the central Pacific by 25 October, by which time a new dipole feature in PV (but not humidity) has formed downstream of the Antarctic Peninsula.

10 Concluding remarks

The splitting of the austral polar vortex at 10hPa in September 2002 was an event the like of which had not previously been observed in the southern hemisphere, yet it was predicted a week or so in advance by ECMWF's operational forecasting system.

Examples have been presented here of the successful prediction of such events in the northern hemisphere, a capability for which was first demonstrated some twenty years ago. The accuracy of stratospheric forecasts has been enhanced in recent years by improvements in observations (with the AMSU-A data available from 1998 onwards), in data-assimilation (for example through introduction of variational techniques (Andersson et *al.*, 1998; Rabier *et al.*, 2000) and direct radiance assimilation (McNally *et al.*, 2000)) and in modelling (such as ECMWF's introduction of 60-level resolution (Untch and Simmons, 1999) and finite-element discretization in the vertical (Untch and Hortal, 2003)). Moreover, medium-range forecasts for the southern hemisphere troposphere have been brought to levels of accuracy similar to those reached for the northern hemisphere troposphere (Simmons and Hollingsworth, 2002). Given that flow conditions in September 2002, however unusual, were conducive to the occurrence of a major break-up of the southern-hemisphere vortex, it would have been surprising had the forecasting system failed to predict this break-up well in advance.

The accuracy of the forecasts discussed in this report is indicative of the high quality of the analyses from which they are run. Analysis error is estimated to be substantially less than radiosonde observation error. A strong control on the large-scale stratospheric analysis is provided by satellite radiance data, and further control may arise from the data-assimilation system's upward propagation of information from the better-observed troposphere. Although radiosonde data do not play a strong direct role in determining the quality of the stratospheric analyses and forecasts for the period examined, they provide valuable information for validation of the forecasting system. They are also important in determining the bias corrections that are applied to the satellite radiance data prior to assimilation. Their importance as part of the long-term climate record has been illustrated by our use of the data to indicate the extreme nature of the warming of late September 2002.

The ERA-40 analyses provide a comprehensive description of the stratosphere from August 1957 onwards, and have been used here to help place the events of September 2002 in historical context. Although these analyses are applicable for a wide range of studies, they should be used with care where observational data are sparse and the assimilating model is prone to systematic error. This is particularly the case for the northern hemisphere upper stratosphere and for the southern hemisphere more generally prior to late 1978, when data first became available from the stratospheric-sounding channels of the MSU, HIRS and SSU instruments on the operational NOAA polar-orbiting satellites. Analyses below 10hPa in the northern hemisphere are much less sensitive to changes in the observing system, and those for January 1958 have been shown to be of sufficient quality to enable good forecasts of the major warming that occurred late in that month.

Acknowledgements We are grateful to Ernst Klinker for providing information on the work of Scherhag, to Tim Palmer for reminding us of the work of Hartmann *et al.* and to Horst Böttger and Tony Hollingsworth for comments on the text. The ERA-40 project is partially funded by the European Union under contract EVK2-CT-1999-00027 and was supported by Fujitsu Ltd through provision of additional computing capacity.

APPENDIX

Access to the rerun analysis data

Readers with direct access to ECMWF's archives can retrieve analysis data at six-hourly intervals from 00UTC on 1 August to 18UTC on 30 September 2002 from the cycle 25r4 rerun including assimilation of data from NOAA-17 by specifying CLASS=RD, EXPVER="ec7s", TYPE=FC, STEP=0 in their MARS retrieval statement. To retrieve data from the rerun from 1 September to 15 October using the more stable advection scheme (without NOAA-17 data), specify EXPVER="eca1". Readers without direct access can order data from ECMWF Data Services, via the ECMWF website (www.ecmwf.int). A specific data set that can be supplied for research use at a nominal handling charge is being prepared for the period 1 August to 15 October. It is based on the first of the above reruns for the month of August, and on the second for the period 1 September to 15 October.

References

Andersson, E., Haseler, J., Undén, P., Courtier, P., Kelly, G., Vasiljevic, D., Brancovic, C. Cardinali, C., Gaffard, C., Hollingsworth, A., Jakob, C., Janssen, P., Klinker, E., Lanzinger, A., Miller, M., Rabier, F., Simmons, A., Strauss, B., Thépaut, J.-N., and Viterbo, P. (1998) The ECMWF implementation of three-dimensional variational assimilation (3D-Var). Part III: Experimental results. *Quart. J. R. Meteorol. Soc.*, **124**, 1831-1860.

Bengtsson, L., Kanamitsu, M., Kållberg, P. and Uppala, S. (1982) FGGE research activities at ECMWF, *Bull. Amer. Meteorol. Soc.*, **63**, 277-303.

Harris, B.A. and Kelly, G.A. (2001) A satellite radiance bias correction scheme for data assimilation. *Quart. J. R. Meteorol. Soc.*, **127**, 1453-1468.

Hartmann, D.L., Palmer, T.N. and Buizza, R. (1996) Finite-time instabilities of lower-stratospheric flow. *J. Atmos. Sci.*, **53**, 2129-2143.

Hortal, M. (2002) The development and testing of a new two-time-level semi-Lagrangian scheme (SETTLS) in the ECMWF forecast model. *Quart. J. Roy. Meteorol. Soc.*, **128**, 1671-1687.

Jung, J.-H., Konor,C.S., Mechoso, C.R. and Arakawa, A. (2001) A study of the stratospheric major warming and subsequent flow recovery during the winter of 1979 with an isentropic vertical coordinate model. *J. Atmos. Sci.*, **58**, 2630-2649.

McNally, A.P., Derber, J.C., Wu, W. and Katz, B.B. 2000 The use of TOVS level-1b radiances in the NCEP SSI analysis system. *Quart. J. R. Meteorol. Soc.*, **126**, 689-724.

Miyakoda, K., Strickler, R.F., and G.D. Hembree (1970) Numerical simulation of the breakdown of a polar-night vortex in the stratosphere. *J. Atmos. Sci.*, **27**, 139-154.

Rabier, F., Järvinen, H., Klinker, E., Mahfouf J.-F. and Simmons, A.J. (2000) The ECMWF operational implementation of four-dimensional variational assimilation. Part I: Experimental results with simplified physics. *Quart. J. Roy. Meteor. Soc.*, **126**, 1143-1170.

Randel, W., Chanin, M.-L., and Michaut, C. (Eds.) (2002) SPARC Intercomparison of middle atmosphere climatologies. SPARC Report No. 3, WCRP-116, WMO/TD-No. 1142, 96pp.

Scherhag, R. (1952) Die explosionsartige Stratosphärenerwärmung des Spätwinters 1951-1952. *Ber. Deut. Wetterdienstes*, **6**, 51-63.

Scherhag, R. (1960) Stratospheric temperature changes and the associated changes in pressure distribution. *J. Meteorol.*, **17**, 575-582.

Simmons, A.J., and Strüfing, R. (1983) Numerical forecasts of stratospheric warming events using a model with a hybrid vertical coordinate. *Quart. J. Roy. Meteorol. Soc.*, **109**, 81-111.

Simmons, A.J., Untch, A., Jakob, C., Kållberg, P. and Undén, P. (1999) Stratospheric water vapour and tropical tropopause temperatures in ECMWF analyses and multi-year simulations. *Quart. J. Roy. Meteorol. Soc.*, **125**, 353-386.

Simmons, A.J. and Hollingsworth, A. (2002) Some aspects of the improvement in skill of numerical weather prediction. *Quart. J. Roy. Meteorol. Soc.*, **128**, 647-677.

Teweles, S. and Finger, F.G. (1958) An abrupt change in stratospheric circulation beginning in mid-January 1958. *Mon. Wea. Rev.*, **86**, 23-28.

Untch, A. and Hortal, M. (2003) A finite-element scheme for the vertical discretization in the semi-Lagrangian version of the ECMWF forecast model. *ECMWF Tech. Memo*, **382**, 32pp.

Untch, A. and Simmons, A.J. (1999) Increased stratospheric resolution in the ECMWF forecasting system. *ECMWF Newsletter*, **82**, 2-8.